Gelsolin Impairs Barrier Function in Pancreatic Ductal Epithelial Cells by Actin Filament Depolymerization in Hypertriglyceridemia-Induced Pancreatitis in Vitro

huiying yang
Guangxi Medical University First Affiliated Hospital https://orcid.org/0000-0002-2185-780X
Zhihai Liang
Guangxi Medical University First Affiliated Hospital
Jinlian Xie
Guangxi Medical University First Affiliated Hospital
Qing Wu
Guangxi Medical University Second Affiliated Hospital
Yingying Qin
Guangxi Medical University First Affiliated Hospital
Shiyu Zhang
Guangxi Medical University First Affiliated Hospital
Guodu Tang (tguodu02@126.com)
Guangxi Medical University First Affiliated Hospital https://orcid.org/0000-0002-2849-3244

Research Article

Keywords: Calcium, gelsolin, actin filament, barrier function, pancreatic ductal epithelial cells, hypertriglyceridemia-induced pancreatitis

Posted Date: May 17th, 2021

DOI: https://doi.org/10.21203/rs.3.rs-504633/v1

Version of Record: A version of this preprint was published at Experimental and Therapeutic Medicine on February 16th, 2022. See the published version at https://doi.org/10.3892/etm.2022.11219.

Abstract

Gelsolin (GSN) is a calcium-regulated actin-binding protein that can sever actin filaments. Actin dynamics affects the function and integrity of epithelial barriers. This study investigated the role of GSN on barrier function in pancreatic ductal epithelial cells (PDECs) in hypertriglyceridemia-induced pancreatitis (HTGP).The human PDEC cell line HPDE6-C7 was silenced for GSN and treated with caerulein (CAE) + triglycerides (TG). Intracellular calcium levels and the actin filament network were analyzed under a fluorescence microscope. The expression of GSN, E-cadherin, nectin-2, ZO-1, and occludin was evaluated by quantitative real-time polymerase chain reaction and western blotting. Ultrastructural changes in tight junctions (TJs) were observed by transmission electron microscopy. The permeability of PDECs was analyzed by fluorescein isothiocyanate-dextran fluorescence. The results showed that CAE + TG increased intracellular calcium levels, actin filament depolymerization, and GSN expression, and increased PDEC permeability by decreasing the expression of E-cadherin, nectin-2, ZO-1, and occludin compared with CAE alone. Moreover, changes in these markers, except for intracellular calcium levels, were reversed by silencing GSN. Based on these results, it can be concluded that GSN disrupts barrier function in PDECs by causing actin filament depolymerization in HTGP in vitro.

Introduction

Severe hypertriglyceridemia (HTG) is the third major cause of acute pancreatitis (AP) after alcohol abuse and cholelithiasis [1]. The severity and complication rates of HTG-induced pancreatitis (HTGP) are higher than those of AP from other etiologies [2] [2]. Although the mechanism by which high triglyceride (TG) levels trigger AP is unknown[3], the toxicity of free fatty acids (FFAs) to the pancreas is the most widely accepted. High concentrations of FFAs are generated from TG hydrolysis by lipases in pancreatic tissues and may trigger the self-digestion of the pancreas by damaging pancreatic acinar cells (PACs) and vascular endothelial cells, activating trypsinogen and protein kinase C, and releasing intracellular calcium[3, 4]. However, few studies on HTGP focused on pancreatic ductal epithelial cells (PDECs).

PDECs are considered the most important component of the pancreatic duct mucosal barrier [5] and play a critical role in preventing the reflux of bile and pancreatic enzymes. Barrier disruption in PDECs may be a major contributor to the occurrence of pancreatitis [6–8]. Moreover, FFAs can destroy the actin filaments of PACs by increasing cytosolic calcium concentrations[9–11], potentially leading to HTGP. However, whether the mechanism underlying HTGP is the same in PDECs and PACs is unknown.

The cytoskeleton is a complex and dynamic system composed primarily of actin filaments and are essential for key cellular functions, including cell adhesion, spreading, migration, and interaction with the environment [12]. Recent studies have shown that the maintenance of the endotheliocyte barrier function and cell-cell junctions is critically dependent on actin filament dynamics[13–16], which is regulated by actin-binding proteins (ABPs) [17].

Gelsolin (GSN) is a calcium-regulated ABP that controls actin dynamics by nucleating, capping, and severing actin filaments and participates in cell morphology, motility, metabolism, apoptosis, phagocytosis[18]. Moreover, previous studies have also showed that GSN is involved in cell-cell junctions and could regulate cell adhesion strenth by remodeling actin[19, 20]. However, the role of GSN in PDECs in HTGP is not fully understood.

In this study, we induced HTGP using caerulein (CAE) and TG and investigate the role of GSN in the regulation of barrier function in PDECs in HTGP in vitro

Materials And Methods

Cell culture and treatment

The human pancreatic ductal epithelial cell line HPDE6-C7 (Guangzhou Jenniobio Biotechnology, Guangzhou, China) was cultured in DMEM medium (Gibco, USA) supplemented with 10% fetal bovine serum (Lonsera, Uruguay), 1% L-glutamine (Solarbio, Beijing, China), and 1% penicillin-streptomycin mixture (Solarbio, Beijing, China) at 37°C in a humidified atmosphere of 5% CO_2. Cells were grown on coverslips (24 mm × 24 mm) in 6-well plates or 25-cm^2 flasks. Cells were silenced for GSN, treated with 100 nM CAE (Sigma-Aldrich, USA) and 2.5 mM TG (T9420, Solarbio, Beijing, China) for 24 h, and divided into 12 groups according to the type of transfection and treatment, as follows: blank control group (BC) (cells without lentiviral transfection), CAE-treated BC group (CAE), TG-treated BC group (TG), CAE + TG-treated BC group (CAE + TG), negative control group (NC) (transfected with an empty vector), CAE-treated NC group (NC + CAE), TG-treated NC group (NC + TG), CAE + TG-treated NC group (NC + CAE + TG), knockdown group (KD) (GSN-silenced), CAE-treated KD group (KD + CAE), TG-treated KD group (KD + TG), and CAE + TG-treated KD group (KD + CAE + TG).

RNA interference-mediated GSN gene silencing

Three pairs of complementary oligonucleotide sequences were designed and synthesized according to GSN CDS sequences. Three double-stranded RNAs converted from complementary sequences were cloned into a pcDNA6.2-GW/EmGFP-miR plasmid vector (R&S Biotechnology, Shanghai, China). The cloned DNA fragments were amplified by PCR and subcloned into the pLenti6.3/V5-DEST vector (R&S Biotechnology, Shanghai, China). The recombinant plasmid and lentiviral packaging mix (Invitrogen; Thermo Fisher Scientific Inc., Waltham, Massachusetts) were transiently co-transfected into 293T cells (R&S Biotechnology, Shanghai, China). Recombinant lentivirus-infected HPDE6-C7 cells with the highest degree of GSN silencing were selected by qRT-PCR screening and validation.

Intracellular calcium measurement

HPDE6C7 cells were grown on 60 mm culture dishes until they reached 60–65% confluence. Cells were washed with Hanks' balanced salt solution without calcium, magnesium, and phenol red (D-HBSS, H1046, Solarbio, Beijing, China) three times and were loaded with Calcium Crimson (C3018, Invitrogen;

Thermo Fisher Scientific, Inc, Waltham, Massachusetts) (5 μM, 1.0 mL per dish) at 37 °C for 30 min in the dark. After that, cells were washed with D-HBSS three times and stained with Hoechst 33258 (H3569, Invitrogen; Thermo Fisher Scientific, Inc., Waltham, Massachusetts) (30 μg/mL, 1.0 mL per dish) at 37 °C for 20 min in the dark. Fluorescence in the cytosol and nucleus was measured at 530–550 nm and 460–495 nm, respectively, under an inverted fluorescence microscope.

Transmission electron microscopy (TEM)

Control and GSN-silenced HPDE6-C7 cells were cultured in 25-cm^2 flasks until they reach 70–80% confluence. Cells were harvested using a cell scraper, centrifuged at 1500 rpm for 10 min, fixed in 3% glutaraldehyde for 2.5 h at 4°C, and washed with PBS (10 mM) three times for 10 min each time. After that, the samples were fixed in 1% osmium for 2 h at 4°C, washed with PBS three times for 10 min each time, dehydrated through a graded ethanol series, embedded in epoxy resin, and cut into 70 nm slices. Samples were stained with 3% uranium acetate-lead citrate. Ultrastructural changes in tight junctions

(TJs) were analyzed by TEM.

Western blotting

Proteins from HPDE6-C7cells were lysed in RIPA buffer (Solarbio, Beijing, China) containing 1% phenylmethylsulfonyl fluoride (PMSF) (Solarbio, Beijing, China) on ice for 30 min and centrifuged at 12,000 rpm at 4°C for 20 min. Protein concentration was determined using a bicinchoninic acid protein assay kit (P0012, Beyotime, Shanghai, China). Proteins were separated by sodium dodecyl sulfate-polyacrylamide gel electrophoresis and electrotransferred onto polyvinylidene fluoride membranes. Membranes were blocked with 5% non-fat milk for 1 h and incubated with primary antibodies against GSN (1:1000, ab74420, Abcam, Cambridge, UK), ZO-1 (1:1000, 21173-1-AP, Proteintech Group, Wuhan, China), nectin-2 (1:1000, ab135246, Abcam, Cambridge, UK), E-cadherin (1:1000, 20874-1-AP, Proteintech Group, Wuhan, China), occludin (1:1000, 27260-1-AP, Proteintech Group, Wuhan, China), and GAPDH (1:10000, ab181602, Abcam, Cambridge, UK) overnight at 4°C, and then incubated with DyLight 680-conjugated secondary anti-rabbit antibody (1:10000, 5366, Cell Signaling Technology) for 1 h at room temperature (RT) in the dark. Immunoreactive bands were imaged using the Odyssey infrared imaging system, and fluorescence intensity was quantified using Image J software.

Quantitative real-time polymerase chain reaction (qRT-PCR)

Total RNA was isolated from HPDE6-C7 cells using RNAiso Plus (9108, TaKaRa Bio Inc, Japan) and converted to cDNA by reverse transcription using PrimeScript RT reagent Kit with gDNA Eraser (RR047B, TaKaRa Bio Inc, Japan). qRT-PCR was performed using TB Green Premix Ex Taq II (RR820B, TaKaRa Bio Inc, Japan) and corresponding primers (Table 1). The relative expression levels of target genes were measured using the $2^{-\Delta\Delta Ct}$ method.

Table 1
Target gene primers used in qRT-PCR

Gene	Forward primer (5’ to 3’)	Reverse primer (5’ to 3’)
GAPDH	ACATCGCTCAGACACCA	GTAGTTGAGGTCAATGAAGGG
GSN	AGCTGGCCAAGCTCTACAAG	TGTTTGCCTGCTTGCCTTTC
E-cadherin	AGGATGACACCCGGGACAAC	TGCAGCTGGCTCAAGTCAAAG
Nectin−2	ACCTGCAAAGTGGAGCATGAGA	CCGGAGATGGACACTTCAGGA
ZO−1	ATAAAGTGCTGGCTTGGTCTGTTTG	GCACTGCCCACCCATCTGTA
Occludin	AGTGCCACTTTGGCATTATGAGA	CTTGTGGCAGCAATTGGAAAC

Immunofluorescence staining of actin filaments

Cells were plated onto coverslips (24 mm × 24 mm) in 6-well plates until they reached 55–60% confluence. The cells were fixed in 4% paraformaldehyde for 15 min at RT, permeabilized in 0.1% Triton X-100 for 5 min, blocked in PBS containing 2% bovine serum albumin (Solarbio, Beijing, China) for 20 min at RT, and stained with tetramethyl rhodamine isothiocyanate-phalloidin (100 nM, 50 μL per well, Solarbio, Beijing, China) for 30 min at RT in the dark. The samples were washed with PBS three times at 5-min intervals between each step and mounted with anti-fading medium containing DAPI (S2100, Solarbio, Beijing, China) for 3 min at RT in the dark. Actin filaments were observed at 530–550 nm, and cell nuclei were observed at 460–495 nm under an upright fluorescence microscope. Images were analyzed using Image J software.

Fluorescein isothiocyanate (FITC)–dextran fluorescence

HPDE6-C7 cell suspensions (2×10^5 cells/transwell) were cultured on microporous polycarbonate membranes (0.4 μm pore size) to full confluence in the upper compartment of 12-well transwell plates (#3401, Corning). The culture medium in the upper compartment was removed, and adhered cells were washed with PBS twice. After that, FITC-dextran (4 kDa, Sigma-Aldrich, USA) (0.5 mg/mL, 500 μL/transwell) was added to the upper compartments, and PBS (1 mL/transwell) was added to the lower compartment. The plates were incubated in the dark for 60 min at 37 °C. Fluorescence in PBS was measured in a microplate reader (excitation, 495 nm; emission, 520 nm) and quantified using a calibration curve of FITC-dextran.

Statistical analysis

The results were expressed as means and SEM. Statistical analysis was performed by one-way analysis of variance using SPSS Statistics version 22.0, GraphPad Prism version 6.0, and Image J. P-values smaller than 0.05 were considered statistically significant.

Results

Effect of intracellular calcium levels on GSN expression in HPDE6-C7 cells treated with CAE and TG

Intracellular calcium was quantified by fluorescence microscopy, and changes in GSN gene and protein expression in HPDE6-C7 cells treated with CAE and TG were analyzed by qRT-PCR and western blotting. The results showed that CAE and CAE + TG increased intracellular calcium levels, and the increase was more pronounced with CAE + TG. TG and GSN silencing had no detectable effect on intracellular calcium levels (Figs. 1A and B). Moreover, CAE and CAE + TG increased the mRNA and protein expression of GSN relative to baseline, and the increase was more pronounced with CAE + TG. TG did not affect GSN expression (Figs. 1C - E).

Effect of GSN on actin filament dynamics in HPDE6-C7 cells treated with CAE and TG

Changes in actin filaments dynamics by GSN silencing were analyzed by immunofluorescence. The results demonstrated that CAE and CAE + TG disrupted the actin filament network, and the effect was stronger with CAE + TG, whereas GSN silencing reduced this effect. TG did not cause actin depolymerization (Fig. 2).

Effect of GSN on the major components of cell-cell junctions in HPDE6-C7 cells treated with CAE and TG

The expression of major components of cell-cell junctions, including E-cadherin, nectin-2, ZO-1, and occludin, was analyzed by qRT-PCR and western blotting. The results showed that CAE and CAE + TG reduced the mRNA and protein expression of these markers relative to baseline, and CAE + TG had a greater effect than CAE (Figs. 3A - D). GSN silencing reduced the effect of CAE and CAE + TG treatment (Fig. 3).

Effect of GSN on TJs ultrastructure and permeability of HPDE6-C7 cells treated with CAE and TG

The ultrastructure of TJs in HPDE6-C7 cells was evaluated by TEM and showed that CAE and CAE + TG treatments decreased the number of TJ strands or disrupted the organization of cell-cell junctions, and some cells in the CAE + TG group had no tight junctions. GSN silencing mitigated this effect in the CAE and CAE + TG groups (Fig. 4A). CAE + TG increased cell permeability more strongly than CAE, and GSN silencing attenuated this effect (Fig. 4B).

Discussion

Previous studies have shown that the disruption of TJs and adherens junctions (AJs) in PDECs plays an important role in the pathogenesis of AP[21, 22]. Moreover, actin filament dynamics is associated with the maintenance of barrier integrity in PDECs [23]. GSN plays a pivotal role in controlling the actin filament network [24]. In in vitro models of HTGP, activated GSN can depolymerize actin filaments and consequently disrupt the barrier function of PDECs. In turn, GSN silencing reduces actin filament

depolymerization and barrier disruption in these cells. Therefore, our results confirm that GSN impairs barrier function in PDECs in vitro by causing the depolymerization of actin filaments in HTGP.

CAE may cause AP by inducing trypsin activation, oxidative stress, and inflammation in the pancreas and has been widely used in animal models of AP[25] [26],and in vitro cell models of AP[27]. Moreover, TGs or their metabolites were used in a cell model of HTGP in vitro[28]. The higher increase in intracellular calcium levels and mRNA and protein expression of GSN in CAE + TG-treated cells than in CAE-treated cells indicated that the increase in GSN level might be up-regulated by excessive calcium in HTGP. However, GSN silencing did not affect calcium levels.

The rearrangement of the actin network can affect the interaction between actin and ABPs [25]. GSN can modulate actin filament structure[24]. In our study, the disruption of actin filaments was more pronounced in HTGP and was reduced by knocking down GSN. Therefore, increased GSN levels and the disruption of actin dynamics in the CAE + TG group indicated that GSN might depolymerize actin filaments in HTGP.

Few studies have evaluated the role of GSN in cell-cell junctions. Our data showed that the decrease in the expression of cell junction proteins was more pronounced in HTGP than in AP, and the expression of these proteins was regulated by GSN. Studies have shown that actin interacts with multiple tight junction proteins, including ZO-1, occludin[29], and adherens junction proteins, such as nectin and E-cadherin[30]. Therefore, in view of the regulatory effect of GSN on actin in HTGP, we hypothesized that GSN regulated the expression of cell junction proteins by actin depolymerization. However, additional studies are necessary to elucidate these interactions.

The endothelial barrier function critically depends on the interactions between cell-cell junction proteins and the actin filament network [31, 32]. However, the role of GSN in epithelial barrier function was only studied in ischemic lung injury [33]. Our results showed that the impairment of TJs in PDECs was more severe in HTGP than in AP and was reduced by knocking down GSN, suggesting that GSN significantly contributed to the maintenance of TJs in these cells. Moreover, the increase in the permeability of PDECs was higher in HTGP than in AP, and this effect was reduced by GSN silencing. Therefore, considering the association between the actin filaments and barrier function[16, 34], we believe that GSN increases cell permeability in HTGP by depolymerizing actin.

Conclusion

GSN impairs epithelial barrier function possibly by causing actin depolymerization in HTGP in vitro. However, additional studies are necessary to investigate the underlying mechanisms and associated signaling pathways.

Declarations

Acknowledgements

The authors are highly thankful to Clinical Experiment Center of the First Affiliated Hospital of Guangxi Medical University for providing necessary facilities for conducting the research work.

Author contributions

Huiying Yang was the main contributor to the research, performed the cell culture, analyzed the data and manuscript writing. Guodu Tang and Zhihai Liang conceived and designed the research. Jinlian Xie and Qing Wu established rat model and prepared the paraffin sections. Yingying Qin collected experimental procedures and ordered experimental reagents. Shiyu Zhang recorded the experimental data. All authors read and approved the final manuscript.

Funding

This study was supported by grants from Guangxi Natural Science Foundation (Grant No.2018GXNSFBA281078) and the National Natural Science Foundation of China (No.81970558).

Conflict of interest

The authors have no conflicts of interest to declare.

Ethics approval

Not applicable.

Data availability

The data used to support the findings of this study are available from the corresponding author upon request.

References

1. de Pretis N, Amodio A and Frulloni L (2018) Hypertriglyceridemic pancreatitis: Epidemiology, pathophysiology and clinical management. United European Gastroenterol J 6:649-655. doi: 10.1177/2050640618755002
2. Yang AL and McNabb-Baltar J (2020) Hypertriglyceridemia and acute pancreatitis. Pancreatology 20:795-800. doi: 10.1016/j.pan.2020.06.005
3. De Pretis N, De Marchi G and Frulloni L (2020) Hypertriglyceridemic pancreatitis. Minerva Gastroenterol Dietol 66:238-245. doi: 10.23736/s1121-421x.19.02641-2
4. Guo YY, Li HX, Zhang Y and He WH (2019) Hypertriglyceridemia-induced acute pancreatitis: progress on disease mechanisms and treatment modalities. Discov Med 27:101-109.
5. Konok GP and Thompson AG (1969) Pancreatic ductal mucosa as a protective barrier in the pathogenesis of pancreatitis. Am J Surg 117:18-23. doi: 10.1016/0002-9610(69)90280-3

6. Quilichini E, Fabre M, Dirami T, Stedman A, De Vas M, Ozguc O, Pasek RC, Cereghini S, Morillon L, Guerra C, Couvelard A, Gannon M and Haumaitre C (2019) Pancreatic Ductal Deletion of Hnf1b Disrupts Exocrine Homeostasis, Leads to Pancreatitis, and Facilitates Tumorigenesis. Cell Mol Gastroenterol Hepatol 8:487-511. doi: 10.1016/j.jcmgh.2019.06.005
7. Hayashi M and Novak I (2013) Molecular basis of potassium channels in pancreatic duct epithelial cells. Channels (Austin) 7:432-441. doi: 10.4161/chan.26100
8. Ishiguro H, Yamamoto A, Nakakuki M, Yi L, Ishiguro M, Yamaguchi M, Kondo S and Mochimaru Y (2012) Physiology and pathophysiology of bicarbonate secretion by pancreatic duct epithelium. Nagoya J Med Sci 74:1-18.
9. Petersen OH, Tepikin AV, Gerasimenko JV, Gerasimenko OV, Sutton R and Criddle DN (2009) Fatty acids, alcohol and fatty acid ethyl esters: toxic Ca2+ signal generation and pancreatitis. Cell Calcium 45:634-42. doi: 10.1016/j.ceca.2009.02.005
10. Bürgin-Maunder CS, Brooks PR and Russell FD (2013) Omega-3 fatty acids modulate Weibel-Palade body degranulation and actin cytoskeleton rearrangement in PMA-stimulated human umbilical vein endothelial cells. Mar Drugs 11:4435-50. doi: 10.3390/md11114435
11. Izadi M, Hou W, Qualmann B and Kessels MM (2018) Direct effects of Ca(2+)/calmodulin on actin filament formation. Biochem Biophys Res Commun 506:355-360. doi: 10.1016/j.bbrc.2018.07.159
12. Svitkina TM (2018) Ultrastructure of the actin cytoskeleton. Curr Opin Cell Biol 54:1-8. doi: 10.1016/j.ceb.2018.02.007
13. Van Itallie CM, Tietgens AJ, Krystofiak E, Kachar B and Anderson JM (2015) A complex of ZO-1 and the BAR-domain protein TOCA-1 regulates actin assembly at the tight junction. Mol Biol Cell 26:2769-87. doi: 10.1091/mbc.E15-04-0232
14. Malinova TS and Huveneers S (2018) Sensing of Cytoskeletal Forces by Asymmetric Adherens Junctions. Trends Cell Biol 28:328-341. doi: 10.1016/j.tcb.2017.11.002
15. Yonemura S (2017) Actin filament association at adherens junctions. J Med Invest 64:14-19. doi: 10.2152/jmi.64.14
16. Shakhov AS, Dugina VB and Alieva IB (2019) Structural Features of Actin Cytoskeleton Required for Endotheliocyte Barrier Function. Biochemistry (Mosc) 84:358-369. doi: 10.1134/S0006297919040035
17. Pollard TD (2016) Actin and Actin-Binding Proteins. Cold Spring Harb Perspect Biol 8. doi: 10.1101/cshperspect.a018226
18. Feldt J, Schicht M, Garreis F, Welss J, Schneider UW and Paulsen F (2019) Structure, regulation and related diseases of the actin-binding protein gelsolin. Expert Rev Mol Med 20:e7. doi: 10.1017/erm.2018.7
19. Chan MWC, El Sayegh TY, Arora PD, Laschinger CA, Overall CM, Morrison C and McCulloch CAG (2004) Regulation of Intercellular Adhesion Strength in Fibroblasts. Journal of Biological Chemistry 279:41047-41057. doi: 10.1074/jbc.M406631200

20. Kim K-m, Adyshev DM, Kása A, Zemskov EA, Kolosova IA, Csortos C and Verin AD (2013) Putative protein partners for the human CPI-17 protein revealed by bacterial two-hybrid screening. Microvascular Research 88:19-24. doi: 10.1016/j.mvr.2013.04.002
21. Kojima T, Yamaguchi H, Ito T, Kyuno D, Kono T, Konno T and Sawada N (2013) Tight junctions in human pancreatic duct epithelial cells. Tissue Barriers 1:e24894. doi: 10.4161/tisb.24894
22. Naydenov NG, Baranwal S, Khan S, Feygin A, Gupta P and Ivanov AI (2013) Novel mechanism of cytokine-induced disruption of epithelial barriers: Janus kinase and protein kinase D-dependent downregulation of junction protein expression. Tissue Barriers 1:e25231. doi: 10.4161/tisb.25231
23. Sakakibara S, Maruo T, Miyata M, Mizutani K and Takai Y (2018) Requirement of the F-actin-binding activity of l-afadin for enhancing the formation of adherens and tight junctions. Genes Cells 23:185-199. doi: 10.1111/gtc.12566
24. Lee M and Kang EH (2020) Molecular dynamics study of interactions between polymorphic actin filaments and gelsolin segment-1. Proteins 88:385-392. doi: 10.1002/prot.25813
25. Kang B, Jo S, Baek J, Nakamura F, Hwang W and Lee H (2019) Role of mechanical flow for actin network organization. Acta Biomater 90:217-224. doi: 10.1016/j.actbio.2019.03.054
26. Hagar HH, Almubrik SA, Attia NM and Aljasser SN (2020) Mesna Alleviates Cerulein-Induced Acute Pancreatitis by Inhibiting the Inflammatory Response and Oxidative Stress in Experimental Rats. Dig Dis Sci 65:3583-3591. doi: 10.1007/s10620-020-06072-1
27. Talukdar R, Sareen A, Zhu H, Yuan Z, Dixit A, Cheema H, George J, Barlass U, Sah R, Garg SK, Banerjee S, Garg P, Dudeja V, Dawra R and Saluja AK (2016) Release of Cathepsin B in Cytosol Causes Cell Death in Acute Pancreatitis. Gastroenterology 151:747-758.e5. doi: 10.1053/j.gastro.2016.06.042
28. Mei Q, Zeng Y, Huang C, Zheng J, Guo Y, Fan J, Fu X, Wang X and Lu Y (2020) Rapamycin Alleviates Hypertriglyceridemia-Related Acute Pancreatitis via Restoring Autophagy Flux and Inhibiting Endoplasmic Reticulum Stress. Inflammation 43:1510-1523. doi: 10.1007/s10753-020-01228-7
29. Odenwald MA, Choi W, Buckley A, Shashikanth N, Joseph NE, Wang Y, Warren MH, Buschmann MM, Pavlyuk R, Hildebrand J, Margolis B, Fanning AS and Turner JR (2017) ZO-1 interactions with F-actin and occludin direct epithelial polarization and single lumen specification in 3D culture. J Cell Sci 130:243-259. doi: 10.1242/jcs.188185
30. Troyanovsky RB, Indra I, Chen CS, Hong S and Troyanovsky SM (2015) Cadherin controls nectin recruitment into adherens junctions by remodeling the actin cytoskeleton. J Cell Sci 128:140-9. doi: 10.1242/jcs.161588
31. McRae M, LaFratta LM, Nguyen BM, Paris JJ, Hauser KF and Conway DE (2018) Characterization of cell-cell junction changes associated with the formation of a strong endothelial barrier. Tissue Barriers 6:e1405774. doi: 10.1080/21688370.2017.1405774
32. Sluysmans S, Vasileva E, Spadaro D, Shah J, Rouaud F and Citi S (2017) The role of apical cell-cell junctions and associated cytoskeleton in mechanotransduction. Biol Cell 109:139-161. doi: 10.1111/boc.201600075

33. Becker PM, Kazi AA, Wadgaonkar R, Pearse DB, Kwiatkowski D and Garcia JG (2003) Pulmonary vascular permeability and ischemic injury in gelsolin-deficient mice. Am J Respir Cell Mol Biol 28:478-84. doi: 10.1165/rcmb.2002-0024OC
34. Bogatcheva NV and Verin AD (2008) The role of cytoskeleton in the regulation of vascular endothelial barrier function. Microvasc Res 76:202-7. doi: 10.1016/j.mvr.2008.06.003

Figures

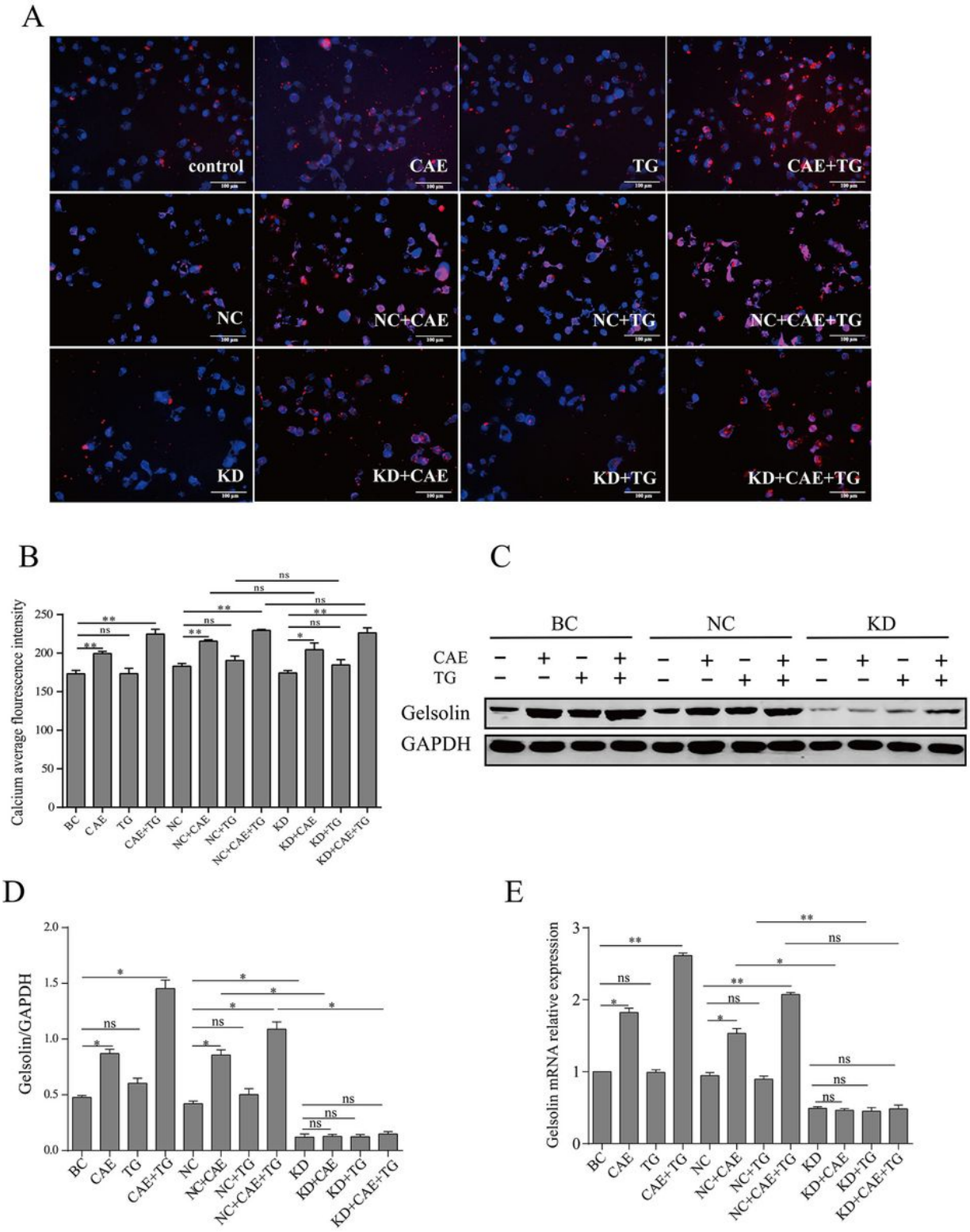

Figure 1

Effect of intracellular calcium levels on gelsolin expression in HPDE6-C7 cells treated with caerulein and triglycerides. (A and B) Changes in intracellular calcium levels in different groups based on fluorescence imaging (×200 magnification) and semiquantitative analysis. (C and D) Protein expression of GSN in different groups by western blotting and semiquantitative analysis. (E) Relative mRNA expression of GSN in different groups by qRT-PCR. Data are means ± SEM, *P<0.05, **P<0.01, nsP>0.05.

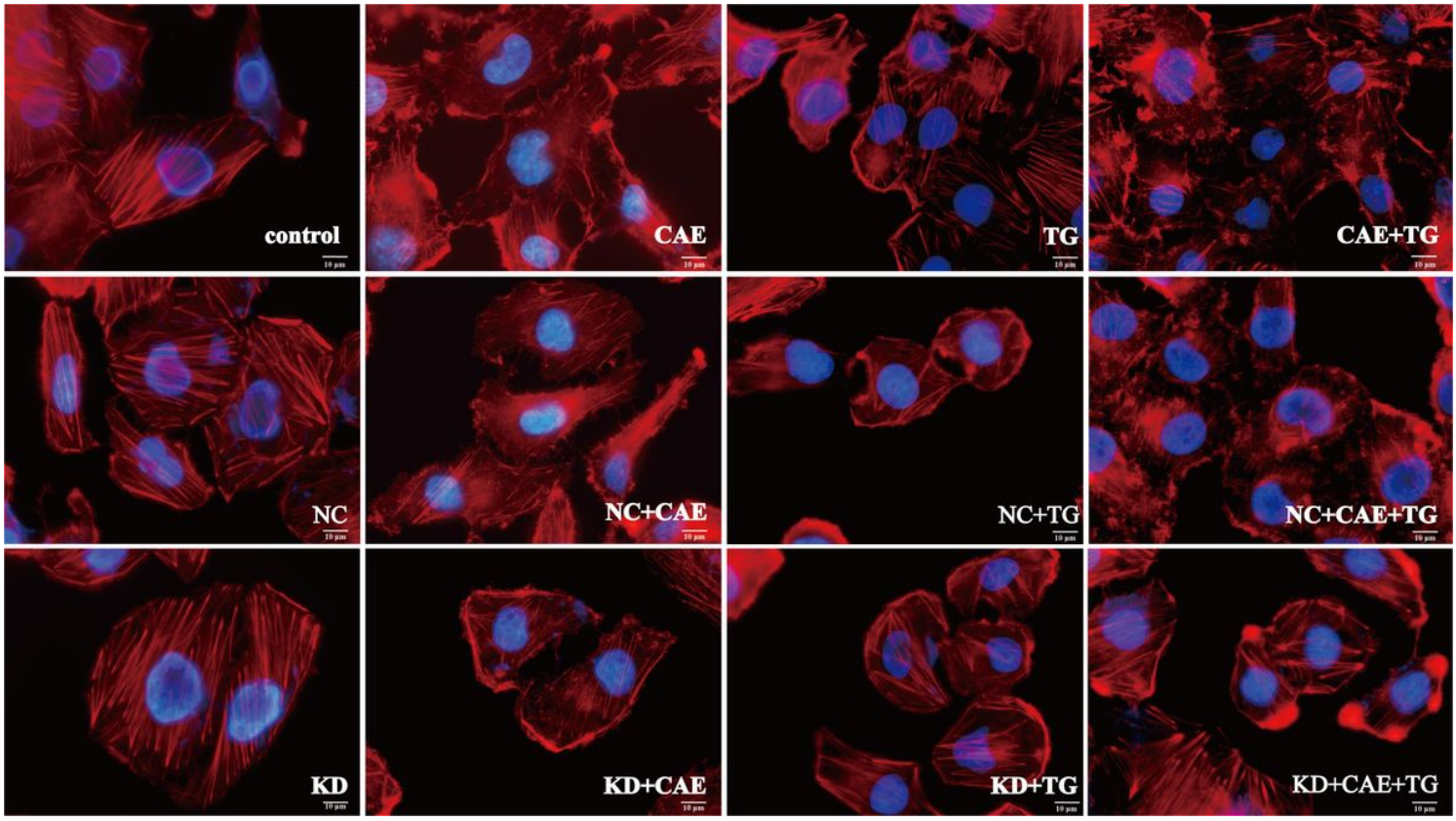

Figure 2

Effect of gelsolin on the dynamics of actin filaments in HPDE6-C7 cells treated with caerulein and triglycerides. The changes in actin filaments by silencing gelsolin were analyzed by tetramethyl rhodamine isothiocyanate-phalloidin immunofluorescence under an upright fluorescence microscope (×1000 magnification).

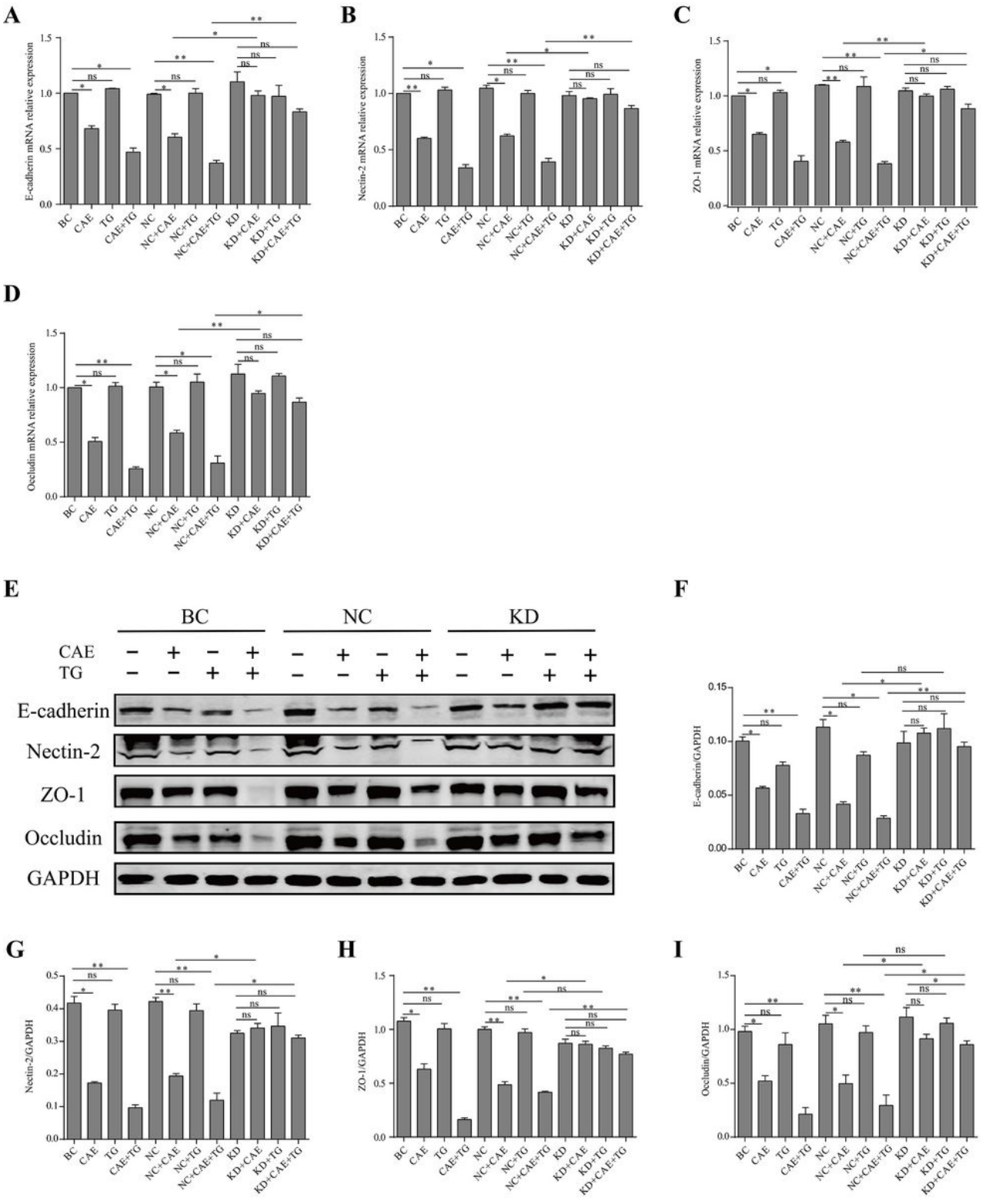

Figure 3

Effect of gelsolin on the major components of cell-cell junctions in HPDE6-C7 cells treated with caerulein and triglycerides. (A - D) Relative mRNA expression of E-cadherin, nectin-2, ZO-1, and occludin by qRT-PCR in different groups. (E - I) Western blot and semiquantitative analyses of the protein expression of E-cadherin, nectin-2, ZO-1, and occludin in different groups. Data are means ± SEM, *P<0.05, **P<0.01, nsP>0.05.

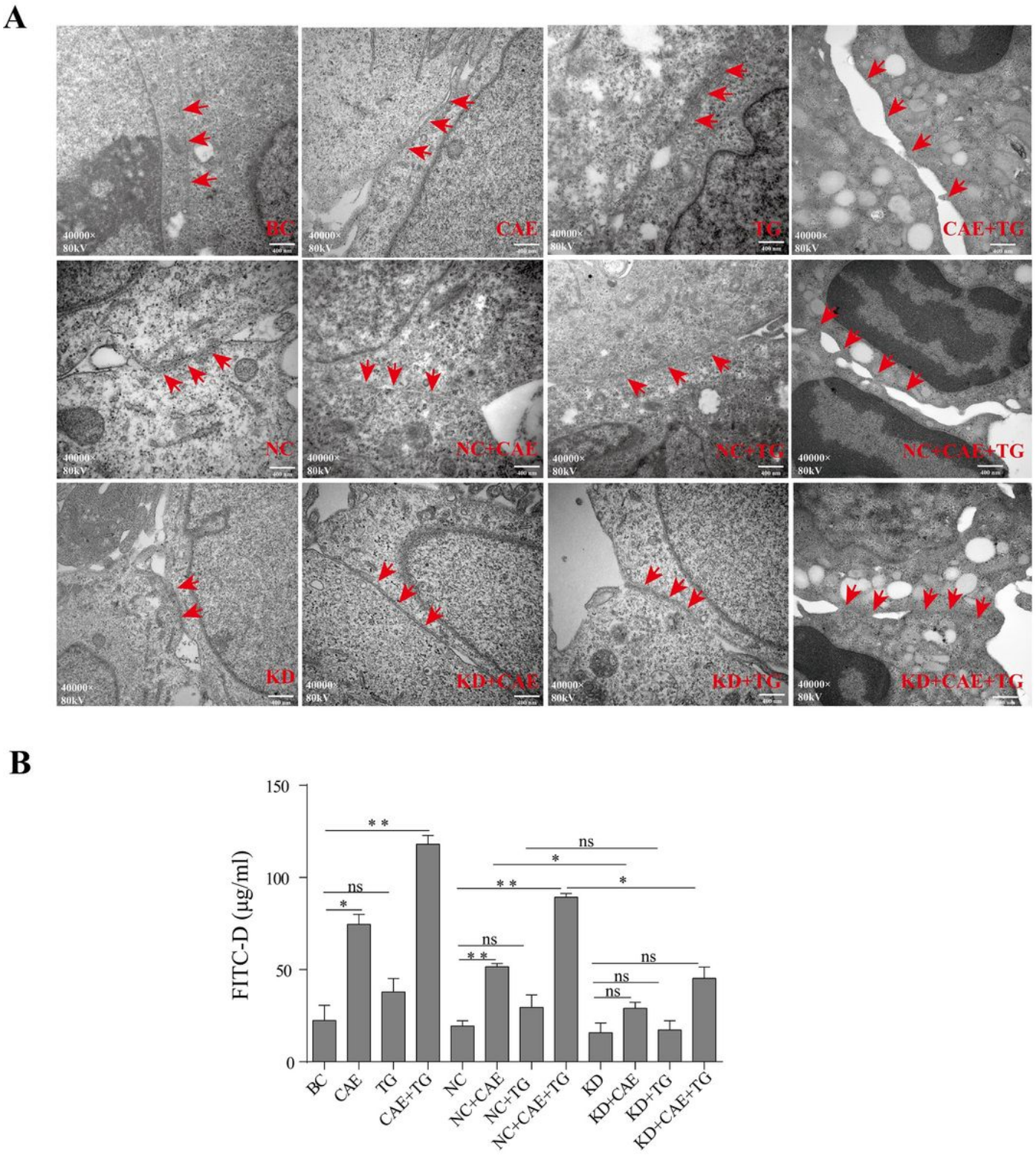

Figure 4

Effect of gelsolin on tight junction ultrastructure and permeability of HPDE6-C7 cells treated with caerulein and triglycerides. (A) Ultrastructure of tight junctions (TJs) by transmission electron microscopy (×40,000 magnification) in different groups (red arrows indicate TJs). (B) Cell permeability analysis by fluorescein isothiocyanate-dextran fluorescence in different groups. Data are means ± SEM, *P<0.05, **P<0.01, nsP>0.05.